Phase shift analysis of all proton-proton scattering data below $T_{lab} = 350$ MeV

J. R. Bergervoet, P. C. van Campen, R. A. M. Klomp, J.-L. de Kok, T. A. Rijken,
V. G. J. Stoks, and J. J. de Swart
*Institute for Theoretical Physics, University of Nijmegen, Nijmegen, The Netherlands**

As a continuation of our 0–30 MeV analysis we present a multienergy phase shift analysis of all pp scattering data below $T_{lab} = 350$ MeV. In the description of all partial waves we take exactly into account the long-range potential consisting of the improved Coulomb potential (including the magnetic moment interaction), the vacuum polarization potential, and the tail of the one-pion-exchange potential. To describe the short-range interaction in the lower partial waves we use a P-matrix parametrization. The intermediate partial waves are treated either by optimal mapping techniques or by using the Nijmegen soft-core potential. The latter gives a better description of the data. The final data set comprises 1626 scattering observables. The best fit to this final data set results in $\chi^2/N_{df} = 1.117$, where $N_{df} = 1576$ is the number of degrees of freedom. The $pp\pi^0$ pseudovector coupling constant is determined to be $f_0^2 = (74.9 \pm 0.7) \times 10^{-3}$. Single-energy phase shifts and errors are also given.

I. INTRODUCTION

The phase-shift analysis of all pp scattering data below $T_{lab} = 350$ MeV presented here, is a continuation to higher energies of our 0–30 MeV analysis.[1] The P-matrix method that was there seen to be very successful in the description of the phase shifts as a function of the energy, is applied here also. The first results of the analysis have already been reported elsewhere.[2,3] In this paper we want to give a full account of the methods and results of the analysis.

From the large, but still finite, number of scattering data one cannot determine an infinite number of phase shifts. However, the long-range part of the interaction is well known, whereas the unknown part of the interaction is sufficiently short ranged as to be screened by the centrifugal barrier. Therefore, all phase parameters with high orbital angular momentum l are well known and we are left with only a finite number of phase shifts to be determined.

With the well-known long-range interaction we mean those effects that are theoretically well understood and that are the same in all realistic descriptions of the pp interaction. We regard as such the tail of the electromagnetic potential, containing the relativistically corrected Coulomb potential[4] (including the magnetic moment interaction), the vacuum polarization potential,[5] and the tail of the one-pion-exchange (OPE) potential. Not all phase-shift analyses include vacuum polarization[6] or Coulomb distortion in the higher partial waves.[6,7]

To give a non-OPE contribution to the partial waves with intermediate angular momentum J, we tried several methods.[3] We used optimal mapping techniques and we also tried to compute them directly via the Nijmegen soft-core (NSC) potential.[8] In all cases an improvement of the description of the data was obtained. The largest improvement was obtained with the NSC potential, which was therefore used in our final fits.

The main difference between this and other multienergy (ME) phase-shift analyses is, that we fully exploit the well-known long-range pp interaction also in the description of the energy dependence of the phase parameters of the *lower* partial waves ($J \leq 4$). This is implemented by using outside some radius $r = b$ a potential tail in the relativistic radial Schrödinger equation. The phenomenology, necessary to describe the precise scattering data accurately, enters the method via the parametrization of a boundary condition at $r = b$ for which we use the P matrix,[9] which is the logarithmic derivative of the radial wave function at $r = b$. In our analysis, phenomenology is therefore only used where there is really a lack of knowledge, i.e., for $r < b$. This method has also an advantage when the long-range interaction is not fully determined and still contains some unknown parameters. These unknown parameters can then be determined from all partial waves. A good example is the OPE potential. The $pp\pi^0$ coupling constant f_0^2 has been determined this way[2] from a preliminary analysis of all pp scattering data below 350 MeV.

In the treatment of the lower partial waves it appeared[3] that with OPE as the only nuclear interaction outside $r = b$, we had to take $b \geq 1.8$ fm in order to get a reasonable description of the data. With intermediate-range forces included in the potential tail, one can take a smaller value for b, the description of the data is better, and the parametrization of the P matrix requires less parameters.[3] Although the description of the intermediate-range part of the nuclear interaction due to multiple-meson exchange or heavier-boson exchange (HBE) is model dependent, different potential models fortunately do agree very well for $r \geq 1.4$ fm. This remarkable feature allows the use of such a potential for $r \geq 1.4$ fm without introducing too much model dependence. Since the tail of the Nijmegen soft-core (NSC) potential model[8] did give a slightly better fit than the tail of the parametrized Paris potential,[10] we chose to include the HBE forces of the

NSC model. With this model for the intermediate-range interaction, the results for the P matrix, which parametrizes the interaction in the inner region, were not satisfactory for the $^1D_2$ and $^1G_4$ partial waves. Therefore, in order to allow for an adjustment of the used HBE potential model to remedy possible imperfections of the intermediate-range forces, the HBE forces for the singlet partial waves were multiplied with an arbitrary parameter, to be determined by the data. For the triplet partial waves such a parameter was not necessary. It should be emphasized that our method for analyzing the scattering data is especially suited to measure the quality of potential tails. In the future more nuclear potential tails will have to be tested in this way.

Our final multienergy fit to the data has $\chi^2/N_{df} = 1.117$. This is considerably lower than other ME phase-shift analyses[6,7] that have $\chi^2/N_{df} \approx 1.3$. Therefore, we think that our ME phase parameters are more in accordance with the data. We also give single-energy (SE) phase shifts and errors. The full error matrices, which take into account the correlation between the phase parameters, and which should be used when adjusting the parameters of a model, are available upon request.

The outline of the paper is as follows. In Sec. II we discuss the method of analysis, based on the parametrization of the P matrix, which is a boundary condition at $r = b$. Some properties of the P matrix are briefly discussed in Sec. III and the treatment of the well-known long-range interaction $(r > b)$ is presented in Sec. IV. Section V describes the data set we used. The determination of the neutral pion-nucleon coupling constant is discussed in Sec. VI, where we also present our multienergy and single-energy results and compare them with other phase-shift analyses.

II. THE METHOD OF ANALYSIS

In previous multienergy (ME) phase-shift analyses various ways of parametrizing the phase parameters as a function of the energy have been employed. The simplest way is used by Bystricky, Lechanoine-Leluc, and Lehar.[6] They express the phase parameters as a polynomial of the energy, multiplied by the OPE phase parameters to insure the correct threshold behavior. For the $^1S_0$ an exception is made; there the effective range approximation is used instead of the OPE phase shift. Arndt, Hyslop, and Roper[7] express the partial-wave amplitude as a sum over one-boson exchange type basis functions, where the masses are chosen as a multiple of the π^0 mass. The strengths of these amplitudes are then fitted to the data. Phase-shift analyses primarily interested in the low-energy region usually use effective range parametrizations or potential parametrizations. The drawbacks of these latter methods are extensively discussed in Ref. 1.

Our method of analysis is about the same as in our 0–30 MeV analysis.[1] What is special about this method? It is that we tried to exploit as much as possible our knowledge about the pp interaction. For large distances the electromagnetic interaction and the OPE part of the nuclear interaction are well known and model indepen-

dent. Concerning the intermediate-range part of the nuclear interaction (say for $r \gtrsim 1$ fm), there is a remarkable agreement between different potential models, despite the fact that there are significant differences in the heavier meson-nucleon coupling constants used, and in the treatment of the two-pion exchange. The short-range part of the nuclear interaction $(r \lesssim 1$ fm) is to a large extent unknown, as can also be seen in the differences between the different potential models.

Therefore, we view the pp interaction as being built up from several parts, which become more well known with larger r. The connection between the unknown inner region and the well-known outer region is implemented via a boundary condition model. The long-range and intermediate-range interactions are incorporated via a potential tail outside $r = b$ in the relativistic radial Schrödinger equation,[11] which is nothing else but a coordinate space version of the relativistic Lippmann-Schwinger integral equation, which in turn is totally equivalent with three-dimensional integral equations, such as the Blankenbecler-Sugar equation.[12] The unknown short-range interaction is parametrized phenomenologically by specifying the P matrix at $r = b$ in each partial wave. The long-range electromagnetic and the OPE potential tails are taken into account exactly. Different models for the intermediate-range forces have been tried. In the final analysis a specific model for these forces has been chosen.

The asymptotic behavior of the radial wave function, which is the solution of the radial Schrödinger equation with specified boundary condition at $r = b$, gives the partial wave S matrix by matching the wave function to Coulomb functions. The S matrix is decomposed into the standard nuclear-bar phase shifts and mixing parameters.[13] For the definition of different kinds of phase parameters, found by matching the radial wave function to functions other than Coulomb functions, see Ref. 1.

For larger angular momentum the inner region becomes less important due to the centrifugal barrier. Therefore, in a phase-shift analysis, one usually parametrizes the lower partial waves only, whereas the higher partial-wave phase parameters are approximated by the OPE phase parameters. The quality of the analysis can be improved significantly if one has a better approximation than OPE for the partial waves with intermediate angular momentum. In a preliminary analysis,[3] we have used the optimal polynomial theory (OPT)[14,15] to give a non-OPE contribution to the phase parameters. There, OPT is only used for the $^1S_0$, $^3P_1$, and $^3P_2$ sequences of partial waves, since in our study of OPT,[3] we found that it could neither predict the mixing parameters nor the $^3F_2$ sequence well enough. Another possibility is to use the heavier boson exchange (HBE) forces of some potential model. In our present analysis we used the HBE forces of the Nijmegen soft-core (NSC) model to give a non-OPE contribution to the phase parameters with intermediate angular momentum.

Given all partial-wave phase parameters, the observables are computed in a standard way.[16,17] The difference of the observables with the experimental data is minimized in a χ^2 fit. Some data are rejected on the basis of

statistical criteria. The number of parameters is determined by the criterion that the fit does not improve significantly when a parameter is added.

In any ME analysis problems can be expected at the end of the energy range. In our analysis, such a problem was most strikingly seen for the $^1S_0$. The $^1S_0$ phase shift showed a tendency to rise at the highest energies. Since it is well known from other phase-shift analyses,[6,7,18−20] that the $^1S_0$ phase shift continues to drop smoothly as a function of energy up to energies far above 350 MeV, we added the $^1S_0$ phase shift at 425 MeV as an extra datum. The value chosen, $\delta(^1S_0) = -19\pm2°$ at 425 MeV, has a sufficiently large error such that it is in agreement with all the aforementioned higher-energy analyses but still insures a proper energy dependence near 350 MeV.

Adjusting all parameters to obtain the χ^2_{min} value gives our final ME fit. The quality of the fit can be seen from the χ^2_{min} value, and from the error matrix of the parameters, which is the inverse of half the second derivative matrix of χ^2_{min} with respect to the parameters.

The energy dependence of the phase parameters in the final ME fit is used in the single-energy (SE) analyses. For the SE analyses we divided the data into ten clusters, from which the SE phase parameters and inverse error matrices were determined. For each phase parameter searched for, we fitted a constant to be added to the energy-dependent P matrix of the ME fit. The results of the SE analyses, i.e., SE phase parameters and error matrices, are a compact representation of the χ^2_{min} surface. They can be used by anyone who wants to adjust the parameters of a model for the pp interaction to the data. Of course, modelists can also compare directly with the data, but this has its disadvantages.[21] Different modelists will pick different sets of data, sometimes perhaps only data that give a low χ^2 value. Comparison of the quality of these models will then be troublesome.

III. THE P MATRIX

A. Definition and properties of the P matrix

We briefly review the definition and properties of the P matrix. For a more detailed discussion, see Ref. 1.

For $r > b$ we use the relativistic[11] radial Schrödinger equation

$$\left[\frac{d^2}{dr^2} + k^2 - \frac{L^2}{r^2} - M_p V(r)\right]\chi(r) = 0 , \tag{1}$$

where $\chi(r)$ is the radial wave function, M_p is the proton mass and L^2 is a shorthand notation for $l(l+1)$, with l the orbital angular momentum. The correct relativistic relation between the center-of-mass (c.m.) relative momentum k and the laboratory kinetic energy T_{lab} is $k^2 = M_p T_{lab}/2$.

The interaction inside $r = b$ is described by a boundary condition at $r = b$, the P matrix

$$P(b;k^2) = b\left[\frac{d\chi}{dr}\chi^{-1}\right]_{r=b} . \tag{2}$$

Given the asymptotic behavior of $\chi(r)$, and the potential $V(r)$ outside $r = b$, the P matrix is uniquely determined.

We add the well-known long-range interaction by means of a potential tail and parametrize the structure of the P matrix as a function of the energy. The potential $V(r)$ we use for $r \geq b$ is discussed in Sec. IV, and the parametrizations for the P matrix are discussed in Sec. III B.

The property of the P matrix on which the parametrizations in this analysis are based is that, if one assumes that a local potential $V(r)$ exists for $r < b$ also, the P matrix can be written as a sum of poles. In the one-channel case we may write

$$P(b;k^2) = c + k^2 \sum_{n=1}^{\infty} \frac{r_n}{k^2 - k_n^2} . \tag{3}$$

For comparison, one might look at the trivial case that $V(r) = 0$ for $r < b$. For the partial wave with orbital angular momentum l this leads to what we call the free P matrix P_{free} for which

$$c = l+1, \quad r_n = 2, \quad k_n = z_n/b , \tag{4}$$

with z_n the nth zero of the spherical Bessel function $j_l(z)$.

In the case that Eq. (1) contains a potential which has a constant value V for $r < b$, this can be absorbed in the k^2 term and we then have

$$P(b;k^2) = P_{free}(b;k^2 - M_p V) . \tag{5}$$

For a coupled-channels P matrix, the residues of Eq. (3) can be factorized. This means that in the neighborhood of a pole one may write

$$P_{ij} = (P_{bg})_{ij} + \xi_i \xi_j \frac{1}{k^2 - k_n^2} , \tag{6}$$

where P_{bg} describes a smooth background. This means that in general the pole will show up in all matrix elements, with residues that are not independent. This is of importance for the choice of the P-matrix parametrization.

The potential that we use will not be entirely exact, since the short-range and intermediate-range forces are not well known and model dependent. Furthermore, our potential tail does not include inelasticities. Therefore, we cannot expect the above properties to hold exactly. The S matrix has a unitarity cut, right-hand cuts due to inelasticities, and left-hand cuts due to particle exchanges. In the P matrix, on the other hand, some of these cuts are removed by including the correct potential tail. Therefore, the P matrix used in our analysis has its nearest left-hand cut at $T_{lab} = -38.83$ MeV. This cut is due to those two-pion exchange effects that are not included in the iterated one-pion exchange or heavier-boson exchange potentials. The lowest-lying right-hand cuts due to the inelasticities and the T_{lab} in MeV of the corresponding thresholds are $pp\pi^0$ (279.6), $d\pi^\pm$ (287.5), and $pn\pi^\pm$ (292.3). One might expect to find some effects of these thresholds at the high end of our energy range. At energies below 400 MeV, however, the inelasticity appears to be still rather small,[6,7,18] so we will neglect it.

An improvement of our model would be the inclusion of the right-hand cuts in some way. This will be necessary if higher energies are to be included.

B. Parametrizations of the P matrix

Many parametrizations of the P matrix can be used to obtain a phenomenological description of the short-range interaction. We start by looking at an uncoupled channel. One could use Eq. (3) and parametrize the P matrix by a finite number of poles. However, this is not the best method if the energy range that is analyzed contains no pole, since in that case a distant pole outside the energy range does not affect the P matrix very much, making it impossible to fit the two parameters r_n and k_n of Eq. (3) to the data. The effect of all the higher poles together can be taken into account by adding a power series in k^2. This leads to

$$P = \frac{k^2 r}{k^2 - k_p^2} + \sum_{n=0}^{N} c_n (k^2)^n \ . \tag{7}$$

A simpler parametrization can be obtained by using no pole at all and keeping only the second term in Eq. (7).

A different parametrization is obtained by starting with P_{free}, the free P matrix, and replacing the argument k^2 by some function $f(k^2)$. If f is expanded in k^2 this leads to the parametrization

$$P = P_{\text{free}} \left[b \, ; k^2 - \sum_{n=0}^{N} a_n (k^2)^n \right] \ . \tag{8}$$

Using Eq. (5) for $r < b$, we see that we have in fact used an energy-dependent potential, independent of r,

$$V(k^2) = \frac{1}{M_p} \sum_{n=0}^{N} a_n (k^2)^n \ . \tag{9}$$

This is the parametrization we use in our final ME fit. Instead of the k^2-dependent but r-independent potential of Eq. (9), one can of course use any short-range potential to parametrize the P matrix.

In the pp interaction we encounter the case of two coupled channels. To describe this coupling, as far as the short-range interaction is involved, we need to construct a 2×2 P matrix. The simplest way to do so starts with two single-channel P matrices as diagonal elements. These can be constructed using one of the methods mentioned earlier. After that one can simply add the off-diagonal elements as some function of k^2, e.g., using a power series

$$P = \begin{bmatrix} P_1 & \displaystyle\sum_{n=0}^{N} d_n(k^2)^n \\ \displaystyle\sum_{n=0}^{N} d_n(k^2)^n & P_2 \end{bmatrix} \ . \tag{10}$$

The P matrix constructed in this way will not have the correct behavior in the vicinity of a pole [see Eq. (6)]. A better construction is

$$P = \begin{bmatrix} \cos\theta & \sin\theta \\ -\sin\theta & \cos\theta \end{bmatrix} \begin{bmatrix} P_1 & 0 \\ 0 & P_2 \end{bmatrix} \begin{bmatrix} \cos\theta & -\sin\theta \\ \sin\theta & \cos\theta \end{bmatrix} \ , \tag{11}$$

where the angle θ is a smooth function of k^2, which can be expanded in a power series. Equation (11) must be used if poles appear in the analyzed energy range. It can also be expected to be better than Eq. (10) if the poles are close to the energy range.

IV. THE POTENTIAL TAIL

The long-range interaction, beyond some distance b, is described by a potential tail. Our objective is to include at least all potentials that can be considered to be model independent.

The electromagnetic interaction is almost the same as in our 0–30 MeV phase-shift analysis;[1] next to the relativistically corrected Coulomb potential $\tilde{V}_C$ (Ref. 4) and the vacuum polarization potential V_{VP},[5] we here have also included the magnetic-moment interaction V_{MM} of the improved Coulomb potential.[4,22] For $T_{\text{lab}} > 30$ MeV vacuum polarization is unimportant. Explicitly, the included electromagnetic potential V_{EM} is

$$V_{\text{EM}} = \tilde{V}_C + V_{\text{MM}} + V_{\text{VP}} = V_{C1} + V_{C2} + V_{\text{MM}} + V_{\text{VP}} \ , \tag{12}$$

with

$$V_{C1} = \frac{\alpha'}{r} \ ,$$

$$V_{C2} = -\frac{1}{2M_p^2} \left[(\Delta + k^2)\frac{\alpha}{r} + \frac{\alpha}{r}(\Delta + k^2) \right] \ , \tag{13}$$

$$V_{\text{MM}} \underset{r \to \infty}{\sim} -\frac{\alpha}{4M_p^2 r^3} \left[\mu_p^2 S_{12} + (6 + 8\kappa_p) \mathbf{L} \cdot \mathbf{S} \right] \ ,$$

where $\alpha' = 2k\eta'/M_p$ with $\eta' = \alpha/v_{\text{lab}}$ the standard Coulomb parameter,[23] Δ is the Laplacian, $\mu_p = 2.792\,847$ is the proton magnetic moment, and $\kappa_p = \mu_p - 1$ is the anomalous magnetic moment.

The magnetic-moment potential is obtained from the phenomenological interaction Lagrangian

$$\mathcal{L}_V = e\bar{\psi}(F_1 i\gamma^\mu A_\mu + F_2 \sigma^{\mu\nu}\partial_\mu A_\nu)\psi \ , \tag{14}$$

where $\sigma^{\mu\nu} = [\gamma^\mu, \gamma^\nu]/2i$, A_μ is the vector-meson (photon) field, and ψ is the proton field. The Dirac and Pauli form factors are given by

$$F_1 = \frac{1 + \mu_p \tau}{1 + \tau} G_E, \quad F_2 = \frac{\kappa_p}{2M_p} \frac{G_E}{1+\tau} \ , \tag{15}$$

where $\tau = -t/4M_p^2$ with t the Mandelstam momentum transfer, and G_E is the Sachs proton electric form factor. Using well-known techniques[11] the one-photon-exchange momentum space pp potential is derived. Introducing the standard momentum dependence for the Sachs form factor as obtained from the dipole fit by Hofstadter and co-workers[24]

$$G_E(t) = \frac{1}{(1 - t/m_D^2)^2} \ ,$$

with $m_D^2 = 0.71$ $(\text{GeV}/c)^2$ the "dipole" mass squared, the potential is Fourier transformed to configuration space. The momentum dependence of the form factors gives rise to short-range Yukawa-like central, spin-spin, tensor, and spin-orbit potentials. The long-range part of the magnet-

ic moment potential is given as in Eq. (13). The contribution of V_{MM} to the scattering amplitude is obtained by summing the potential integrated with Coulomb functions for each partial wave up to $l = 1000$, since one should use the Coulomb distorted-wave Born approximation (CDWBA) rather than the plane-wave Born approximation (BA) in calculating the pp magnetic-moment scattering amplitude. This was already pointed out by Knutson and Chiang.[25] The spin-orbit part of the interaction, however, gives rise to a term that converges too slowly for a summation on a computer to be practical. Fortunately, this part can be summed analytically (see also Ref. 25). A more detailed account of our treatment of the magnetic-moment interaction in our phase-shift analysis will be published elsewhere.[22]

The longest-range nuclear potential, one-pion ex-change, is included as

$$V_{OPE} = \frac{1}{3} f_0^2 \left[\frac{m}{m_c} \right]^2 \frac{M_p}{E} \frac{e^{-mr}}{r}$$

$$\times \left[(\sigma_1 \cdot \sigma_2) + S_{12} \left[1 + \frac{3}{(mr)} + \frac{3}{(mr)^2} \right] \right] , \qquad (16)$$

where m is the π^0 mass, m_c is a scaling mass, conventionally chosen to be the charged pion mass,[26] and $E = (M_p^2 + k^2)^{1/2}$ with k the c.m. relative momentum. No form factor has been included, since the latter represents a short-range effect, whereas the potential is used for $r > b$ only. The $pp\pi^0$ pseudovector coupling constant $f_0^2 \equiv f_{pp\pi^0}^2 / 4\pi$, appearing in this potential, is left as a free parameter. It determines the strength of the Yu-

TABLE I. Data reference table. A dagger denotes data not included in the Nucleon-Nucleon Scattering Data Tables (Refs. 121 and 122). An asterisk denotes data not included in the data set NN896 of SAID (Ref. 123).

T_{lab} (MeV)	No.[a] type	χ^2	% error	Predicted norm[b]	Reject	Reference	Comment
0.33766− −0.40517	6 σ	3.852	float[c]	1.3222	0.372 83 MeV	27	d
0.35003− −0.42003[†]	36 σ	39.194	float[c]	0.9975		28	e
0.35009[†]	17 σ	25.172	0.16	0.9993		28	e
0.40004[†]	3 σ	1.033	0.21	1.0009		28	
0.42006[†]	22 σ	38.545	0.16	0.9995		28	e
0.49923[†]	39 σ	32.020	0.16	0.9989		28	e
0.49925[†*]	3 σ		0.09		all	29	f,g
0.74996[†]	26 σ	16.825	0.16	0.9987		28	e
0.99183[†]	31 σ	25.475	0.16	0.9989		28	e
0.9919[†*]	3 σ		0.09		all	29	f,g
0.9919[†*]	2 σ		float[c]		all	30	f,g
1.397	11 σ		none		all	31	f
1.855	13 σ		none		all	31	f
1.8806[†*]	3 σ		0.09		all	29	f,g
2.425	14 σ		none		all	31	f
3.037	13 σ		none		all	31	f
4.978	17 σ	17.272	0.4	1.0029		32	
5.05[†]	11 P	5.284	1.0	0.9980		33	
6.141[†*]	17 σ		0.4		all	34	h,i
6.141[†*]	6 P		none		all	35	j
6.968	17 σ	15.922	0.4	1.0051		32	
8.030	17 σ	12.128	0.4	1.0051		32	
8.097	16 σ		0.4		all	34	h,i
9.57[†]	1 A_{yy}	0.234	none			36	
9.6[*]	5 P	2.172	none			37	k
9.69	26 σ	18.651	0.73	0.9853		38	l,m
9.69	5 σ	5.476	(0.36)	0.9819		39	n
9.85[†]	15 P	17.381	1.0	0.9956		33	
9.918[*]	17 σ		0.4		all	34	h,i
9.918	11 σ	19.902	0.38	0.9959	20.05°	39	
10.00	7 P	9.684	none			40	
11.40	1 A_{yy}/A_{xx}	0.083	none			41	
13.60	11 σ	15.468	0.33	1.0024		39	
14.16	17 σ		none		all	42	j,l
15.6[*]	5 P	1.679	none		36.14°	37	k

TABLE I. (*Continued*).

T_{lab} (MeV)	No.ᵃ type	χ^2	% error	Predicted normᵇ	Reject	Reference	Comment
16.2	1 P	0.679	none			43	1
17.7*	1 P	0.328	none			44	
19.15−−26.50	3 A_{xx}, 3 A_{yy}	2.484	floatᶜ	1.0147		41	
19.7⁺*	13 σ	8.482	0.37	0.9987		45	
19.7*	6 P		none		all	37	k,o
19.8*	15 σ	22.039	none			46	
19.84*	7 σ	8.608	none			47	p
20.00*	1 C_{nn}	1.131	none			48	
20.20	8 P		12.0		all	49	j
21.95−−50.02	7 σ		0.36		all	50	o
25.63	23 σ		0.93		all	51	j
27.05	1 C_{nn}	0.309	none			52	
27.4*	1 P	0.144	none			53	q
27.6	3 R, 3 A	13.078	3.0	1.0340		54	
28.16	1 σ	0.731	none			55	1
30.0	2 P	4.498	4.0	1.0068		56	
31.15	1 σ	0.002	none			55	1
34.20	1 σ	0.886	none			55	1
36.8*	2 P	0.417	none			53	q
36.90	1 σ	0.198	none			55	1
37.23	1 A_{xx}, 1 A_{yy}	1.123	floatᶜ	1.0325		57	
38.3*	1 P	2.997	none			53	q
39.4	27 σ	31.327	0.93	1.0080		58	1
39.60	1 σ	0.209	none			55	1
41.0	1 σ	0.814	none			59	
44.66	1 σ	1.249	none			55	1
46.0−−86.0*	5 σ		floatᶜ		all	60	o
46.0	1 P	1.244	2.8	1.0017		60	r
46.9⁺*	1 A_{xx}, 1 A_{yy}	0.025	floatᶜ	1.0711		61	
47.5	1 A_{xx}, 1 A_{yy}	2.673	floatᶜ	1.2531		62	
47.5	5 A	7.123	5.0	1.0178		63	
47.8	5 R	5.116	5.0	0.9977		54	
47.8	5 A	2.434	5.0	0.9809		54	
49.41	30 σ	31.164	0.32	1.0011	14.02°, 17.06°	64	
49.7*	1 P	8.257	none			53	q
49.9	2 P	0.008	3.0	1.0005		56	
50.0	1 D	1.534	none			65	
50.06⁺*	24 σ	12.823	1.6	0.9820		66	
50.17	1 σ	0.487	none			55	1
51.5	1 σ	0.869	none			59	
51.7	1 P	0.482	none			53	q
52.0	1 A_{yy}, 1 C_{kp}	5.406	none			67	
52.34	29 σ	23.663	0.53	1.0037	16.22°, 18.24°, 20.27°	68	
52.34⁺	12 P	7.643	2.0	0.9846		69	
53.2	1 P	1.412	none			53	q
56.0	1 P	0.317	2.8	1.0032		60	r
56.15	1 σ	0.241	none			55	1
58.5	1 P	0.538	none			53	q
61.92	1 σ	0.012	none			55	1
66.0	11 σ		floatᶜ		all	60	j
66.0	11 P	8.323	2.8	0.9769		60	r
68.19⁺	12 P	6.533	2.0	0.9826		69	
68.3	26 σ	30.733	1.1	0.9923		70	1
68.42	1 σ	0.006	none			55	1
69.5	1 σ	0.037	none			59	

TABLE I. (*Continued*).

T_{lab} (MeV)	No.[a] type	χ^2	% error	Predicted norm[b]	Reject	Reference	Comment
70.0*	5 σ	9.471	float[c]	5.7558	25.0°	59	
70.0	1 P	2.031	none			53	q
71.0	1 P	0.465	2.8	1.0040		60	r
73.5	1 A_{yy}	0.704	none			71	
78.0	1 P	0.552	2.8	0.9935		60	r
78.5	1 σ	0.003	none			59	
86.0	1 P	0.014	2.8	1.0012		60	r
95.0	1 σ	0.016	none			59	
95.0	6 σ	2.318	none			59	
95.0	5 σ	3.820	float[c]	4.6381	25.0°	59	
95.0	14 σ	5.742	float[c]	1.0287		60	
95.0	14 P	13.445	2.8	1.0082		60	r
97.0	1 P	2.329	none			53	q
97.7	13 P	14.303	0.85	1.0092		72	
98.0*	14 σ		4.5		all	73	o
98.0	14 P	13.287	2.2	1.0225		73	s
98.0*	5 P	4.634	3.0	1.0058		74	t
98.0*	3 P	6.273	3.0	1.0365		74	u
98.0	5 D	7.596	3.0	1.0046		74	
98.0	1 A_{yy}	0.013	none			71	
98.1	5 R	6.424	none			75	
98.1	4 R,R'	1.168	none			75	v
98.8	19 σ	16.399	1.0	0.9948		72	
102.0	3 σ	7.565	float[c]	1.0122		60	
102.0	3 P	1.940	2.8	0.9816		60	r
107.0	3 σ	1.167	float[c]	1.0722		60	
107.0*	3 P	7.234	2.8	1.0146		60	r
118.0	16 σ	23.673	float[c]	1.0448	86.8°	60	
118.0*	16 P	31.718	2.8	1.0507		60	r
127.0	3 σ	0.766	float[c]	1.0400		60	
127.0*	3 P	8.247	2.8	1.0171		60	r
130.0	4 P	3.059	3.3	1.0197		76	
137.0	3 σ	0.023	float[c]	1.0120		60	
137.0	3 P	3.524	2.8	1.0279		60	r
137.5	5 R'	1.123	5.0	0.9993		77	
138.0*	17 P	25.717	none		82°, 86°	78	w
138.0	4 D	3.986	none			78	w
139.0	6 A	3.929	4.0	1.0439		79	
140.4	6 R,R'	6.755	none		72.1°	80	v
140.5	6 R	4.263	none			81	x
140.7	20 P	19.053	0.85	0.9970		82	
141.0	8 R	10.139	none			83	
142.0*	20 σ		4.5		all	73	o
142.0	29 P	29.356	2.2	0.9544	6.23°, 78.05°	73	s
142.0*	8 P		3.0		all	84	u,o
142.0*	8 P	7.049	3.0	1.0016		84	t
142.0	8 D	11.279	3.0	1.0008		84	
143.0	7 P	5.102	none			85	
143.0	7 D	7.444	none			85	
143.0	6 A	4.886	none			86	
143.2	1 P	1.881	none			71	
143.2	2 A_{yy}	0.304	none			71	
144.0	27 σ	36.142	0.58	0.9936	7.26°	87	
144.1	6 σ	3.042	0.88	0.9944		82	
144.1	15 σ	31.931	0.56	0.9861		82	
147.0*	3 σ	1.332	float[c]	0.9955		60	
147.0*	12 σ	20.947	float[c]	0.8526	4.13°	60	
147.0*	15 σ	9.151	float[c]	0.9263		60	
147.0*	11 σ	7.360	float[c]	0.9251		60	

TABLE I. (*Continued*).

T_{lab} (MeV)	No.[a] type	χ^2	% error	Predicted norm[b]	Reject	Reference	Comment
147.0*	1 σ	1.004	none			88	
147.0	3 P	1.635	2.8	0.9946		60	r
147.0	12 P	16.225	2.8	1.0042		60	r
147.0	15 P	14.942	2.8	0.9933		60	r
147.0	13 P	22.975	2.8	0.9908		60	r
156.0	24 σ	24.692	none		8.3°, 25.0°	89	
170.0	6 σ	10.412	6.9	1.0674	10.1°	90	
170.0	5 P	3.450	6.6	1.0510		91	
170.0	7 P	2.760	3.3	1.0154		76	
174.0*	7 σ		6.9		all	90	o
176.0 − −179.0*	2 P	1.452	3.7	0.9769		92	
203.6*	3 σ	10.778	5.4	1.0138		93	
205.0	1 P	1.705	none			94	
209.1	3 P	2.578	2.8	0.9924		95	v
209.1	3 D	8.160	2.8	0.9782		95	y
209.1	3 R	0.559	2.8	0.9962		95	y
209.1	1 R'	1.700	2.8	1.0181		95	y
210.0[†]	7 σ	6.855	1.64	1.0174		96	
210.0*	2 P	2.680	none			97	z
210.0*	9 P	8.747	3.3	0.9912	67.8°	76	aa
210.0	7 P	1.905	3.6	1.0065		98	bb
213.0	13 σ	10.576	1.3	0.9978	8.9°, 9.8°	99	
213.0	13 P	23.508	3.1	1.0030		99	cc
213.0*	7 P	14.249	none		90.0°	100	dd
213.0*	7 P	12.001	none		90.0°	100	dd
213.0*	7 P	8.664	none		90.0°	100	dd
213.0	7 D	6.637	none			100	
213.0	7 R	2.846	none			101	ee
213.0	5 A,R	3.111	none			101	ff
213.0	2 A	1.331	none			96	
213.0	7 R,R'	13.364	none		60.0°	102	v
217.0	7 P	12.719	2.2	1.0360		98	
225.0	1 P	0.932	none			94	
241.0	8 P	18.797	3.0	0.9878		103	
241.0	8 D	18.405	4.0	0.9470		103	
241.0	8 D_t		7.0		all	103	j
241.0	8 R,R'	3.319	4.0	0.9586		103	v
241.0	8 A,A'	13.003	4.0	0.9982		103	gg
241.0	8 $M_{\omega 0sn}$	9.274	8.0	1.0144		103	hh
241.0	8 $M_{\omega 0kn}$	8.511	8.0	0.9847		103	ii
259.0	6 σ		5.2		all	90	o
260.0*	6 σ	5.535	5.2	0.9867	9.3°	90	
266.0	1 P	0.483	0.4	1.0006		104	
276.0	6 P	8.064	7.5	1.1213		105	
285.0	22 σ	25.886	float[c]	1.0348		106	
300.0[†]	1 σ	2.448	1.8	0.9737		107	
302.9[†]	10 A_{zz}	15.307	2.0	0.9888		108	jj
305.0	14 C_{nn}	16.864	8.0	1.1432		109	
307.0	7 P	8.491	3.0	1.0050	83.7°	110	
308.0	1 P	0.013	none			94	
310.0	6 D	6.881	none			105	
310.0	6 R	9.778	none			105	
312.0	13 P	19.372	0.6	1.0018		111	
312.0	13 D	7.849	1.2	0.9987		111	
312.0	13 R	13.706	1.2	0.9997		111	
312.0	13 A	7.729	1.2	1.0012	4.32°	111	
314.0	8 P	17.414	3.0	0.9381		103	
314.0	8 D_t	2.002	7.0	1.0357		103	

TABLE I. (*Continued*).

T_{lab} (MeV)	No.[a] type	χ^2	% error	Predicted norm[b]	Reject	Reference	Comment
314.0	8 R, R'	7.786	4.0	0.9520		103	v
314.0	8 A, A'	10.176	4.0	1.0797		103	gg
314.0	8 $M_{\omega 0sn}$	3.992	8.0	0.9977		103	hh
314.0	8 $M_{\omega 0kn}$	2.611	8.0	0.9842		103	ii
315.0	7 σ	6.086	10.0	1.0282		105	
315.0	7 P	8.142	4.0	1.0743		105	
315.0	1 A_{yy}	0.414	none			112	
315.0	1 A_{yy}, 1 C_{kp}	0.039	none			113	
316.0	3 A	0.580	none			114	
318.0[†]	1 P	0.075	1.0	0.9982		115	
320.0	1 P	0.002	0.4	1.0000		104	
320.0	1 C_{nn}	1.158	none			116	
324.0 − −327.8	4 P	1.742	1.5	0.9924		95	y
324.0	3 P	2.341	1.5	0.9997		95	y
324.0	3 D	3.185	1.5	0.9904		95	y
324.0	3 R	1.332	1.5	1.0042		95	y
324.0	1 R'	3.715	1.5	1.0084		95	y
325.0[†]	19 σ	25.087	10.0	1.0239		117	
327.0	1 P	0.676	none			94	
328.0	5 σ	8.748	2.9	0.9635		93	
328.0	14 P	6.667	6.2	1.0201	85.3°	118	
330.0	13 C_{nn}	4.675	8.0	1.0705		109	
332.5	12 σ	17.339	(3.0)	1.1358		119	n
334.5	10 σ	7.381	none			120	
334.5	11 P	11.323	6.0	1.0642		120	
341.0	16 P	20.506	3.0	0.9978		103	
341.0	16 D	20.244	4.0	0.9521		103	
341.0	16 R	11.661	4.0	0.9659	74.0°	103	
341.0	16 A	20.871	4.0	0.9604		103	
348.0	22 σ	20.343	float[c]	1.0092		106	
350.0[†]	1 σ	1.027	1.8	1.0179		107	

[a]The number includes all published data.

[b]Predicted norm with which the experimental values should be multiplied before comparison with the theoretical values.

[c]Floated normalization because these data are relative only.

[d]0.372 83 MeV rejected. This is in accordance with the result of the phase-shift analysis of Sher, Signell, and Heller (Ref. 124).

[e]Two extra angle-dependent normalizations included (see Ref. 28).

[f]Rejected as a result of the analysis of van der Sanden, Emmen, and de Swart (Ref. 125) of the 0–3 MeV data.

[g]The authors of Ref. 28 call these data doubtful, mainly because of the use of the current integration method, which they found unsatisfactory at low energies.

[h]Disagreement between single-group fit and ME fit too large.

[i]We used the BGS data (see Ref. 34).

[j]Group rejected due to improbably low χ^2 (rejection criteria).

[k]Numerical values were taken from the Nucleon-Nucleon Scattering Data Tables (Ref. 121).

[l]Probable errors changed to standard errors ($\sigma \approx 1.48$ probable errors).

[m]Normalization error extracted from absolute error and relative error (see Ref. 38).

[n]Floated normalization because norm contributes more than 9 to χ^2.

[o]Group rejected due to improbably high χ^2 (rejection criteria).

[p]Overall error taken (see Ref. 47).

[q]Renormalized according to Jarvis and Rose (Ref. 126): polarization times 0.89, error unchanged.

[r]Renormalized according to Jarvis and Rose (Ref. 126): polarization times 0.933, error unchanged.

[s]Renormalized according to Jarvis and Rose (Ref. 126): polarization times 0.911, error unchanged.

[t]Analyzing power measurement.

[u]Asymmetry measurement.

[v]Measured was $R \cos(\theta) + R' \sin(\theta)$.

[w]Renormalized according to Michalowicz (Ref. 89) by a factor of 0.85.

<div align="center">TABLE I. (*Continued*).</div>

[x]Total error taken (see Ref. 81).

[y]Numerical values from Bugg and co-workers (Ref. 19).

[z]Measurement of polarization and analyzing power as a check for time-reversal invariance. We do not discriminate between them.

[aa]We used the C-H$_2$ data in accordance with the data at 130 and 170 MeV.

[bb]Renormalized according to Thorndike (Ref. 96): polarization times (0.985 ± 0.035).

[cc]Renormalized according to Thorndike (Ref. 96): polarization times (0.970 ± 0.030).

[dd]Datum at 90° not included, as recommended by the authors of this measurement (see Ref. 100).

[ee]Revised values from Thorndike (Ref. 96).

[ff]Measured was $A \cos(\theta) + R \sin(\theta)$.

[gg]Measured was $A \cos(\theta) + A' \sin(\theta)$.

[hh]Measured was $\cos(\omega)M_{s'0sn} - \sin(\omega)M_{k'0sn}$ in the four-index notation as used in Ref. 127.

[ii]Measured was $\cos(\omega)M_{s'0kn} - \sin(\omega)M_{k'0kn}$ in the four-index notation as used in Ref. 127.

[jj]Normalization error from error in beam polarization and target polarization (see Ref. 108).

kawa tail, so it represents the coupling constant at the pion pole. The contributions of the long-range potentials V_{EM} and V_{OPE} to the scattering amplitude are calculated in CDWBA.

The intermediate-range forces cannot be included without introducing some model dependence. Therefore, we first did not include any nuclear potential tail other than OPE. A reasonable fit was then only possible for $b \geq 1.8$ fm. When we[3] used the intermediate-range forces of the Nijmegen soft-core potential[8] or the parametrized Paris potential,[10] b could be chosen smaller and the fit to the data became better, even if less parameters were used for the short-range interaction. These potentials were used in our model after removing their OPE part, keeping only what we call "intermediate-range forces." In all cases we kept the OPE potential of Eq. (16). Since the fit to the data with the Nijmegen intermediate-range forces was somewhat better than with the Paris intermediate-range forces,[2] we chose to include the non-OPE part of the Nijmegen potential in our potential tail for our final ME fit.

Although an improved fit was obtained in this way, there were still indications that this potential tail was not perfect. This was most clearly seen in the $^1D_2$ and $^1G_4$ partial waves. The potential in the inner region, which is the equivalent of the P matrix, appeared to be highly attractive for these waves. This points towards an incorrect potential tail. This is because of the fact that the region $r < b$ has only little influence on the phase shifts for higher l, so in order to compensate for rather small imperfections in the potential tail, very large short-range potentials are needed. To investigate this we multiplied the intermediate-range potential by the factor f_{med}, which allows for an adjustment of the used potential model to remedy possible imperfections of the intermediate-range forces. This parameter f_{med} makes the tail of the potential more attractive, so one needs less exorbitant attraction in the inner region. The non-OPE part of the Nijmegen potential (V^N_{HBE}) is multiplied for the singlet waves with this factor, now called f^s_{med}. The best fit was achieved with $f^s_{med} \approx 1.6$. For the triplet waves such a parameter turned out to be unnecessary (i.e., $f^t_{med} \approx 1.0$).

Summarizing, the employed potential tail V_L is

$$V_L = V_{EM} + V_{NUC} = V_{EM} + V_{OPE} + V^N_{HBE}(f^s_{med}), \qquad (17)$$

and contains two parameters, f^2_0 and f^s_{med}. In our final fit f^s_{med} was fixed at 1.6 to save computer storage and time, whereas f^2_0 was still left as a free parameter.

V. THE DATA

A list of all groups of data we used in our analysis is shown in Table I. Although most of these data already have been presented in previous analyses[6,18,19,128–131] we give them here explicitly, since we wish to provide a self-contained and complete data base for our future phase-shift analyses.

Our data set consists of all pp scattering data below $T_{lab} = 350$ MeV, published in a regular physics journal as of 1955 (we therefore rather arbitrarily do no longer include the Princeton54 cross-section data of Yntema and White,[132] which were published in 1954, although they were included in our 0–30 MeV analysis[1]), and is updated up to August 1989. A detailed list of the major part of the data can be found in the Nucleon-Nucleon Scattering Data Tables of Bystricky and Lehar[121,122] as published in 1978 and 1981. For all experimental results we have consulted the original references and we corrected for some minor printing errors in the Scattering Data Tables. Moreover, we include data groups that are not contained in these tables (e.g., because they were published after 1981). These groups are denoted by a dagger. Groups of data that are not included in the latest data set NN896 of SAID (Ref. 123) are denoted by an asterisk.

On the other hand, we do not include dispersion relation predictions[133] and data that were obtained from quasielastic scattering (e.g., deuteron targets). Total cross-section data (σ_{tot}, $\Delta\sigma_T$, $\Delta\sigma_L$) were omitted because of the difficulties of their definition and because of the differences in the treatment of the Coulomb-nuclear interference term by the experimentalists. As in our 0–30 MeV analysis,[1] we also do not include data that have not been published (yet) or that have only been reported in conference proceedings. The main difference between our data base and that of other analyses[6,7,18] is that we have extended the energy range downwards to 0 MeV and included all low-energy data. The data set up to 30 MeV is almost the same as in our 0–30 MeV analysis.[1]

TABLE II. The neutral pion-nucleon coupling constant $10^3 \times f_0^2$.

MacGregor et al. (Ref. 128)	1968	81.4 ± 4.6
Bugg (Ref. 134)	1968	75.2 ± 3.9
Breit et al. (Ref. 135)	1971	$73.1 - 81.8$
Bugg et al. (Ref. 19)	1978	77.8 ± 3.6
Kroll (Ref. 133)	1981	80.3 ± 2.2
Present result	1989	74.9 ± 0.7

However, we added one polarization measurement,[44] one spin correlation,[48] and 22 cross-section data,[46,47] which were found to be missing from our previously published analysis of the pp scattering data below $T_{lab} = 30$ MeV.

Starting with this set of 1917 scattering observables, the P-matrix parameters and the neutral pion-nucleon coupling constant were adjusted to obtain a χ^2_{min}. Data that were more than 3 standard deviations (3σ) off were rejected and the parameters were adjusted again. If the experimental normalization on a group of data contributed more than 9 to χ^2, these data were floated (freely renormalized) by us, which is indicated by "n" in the column labeled "Comment" in Table I. The original experimental normalization error is shown in parentheses for such cases. Groups that had an improbably low or high χ^2 were rejected also. Groups rejected this way are indicated by "j" and "o," respectively, in the column labeled "Comment."

If we compare with our 0–30 MeV analysis,[1] we note that the Berkeley67 polarization data of Slobodrian et al.[37] are no longer rejected, except for the six polarization data at 19.7 MeV that still have a χ^2 that is too high. All other changes in the data set below $T_{lab} = 30$ MeV result in the same data set as used in our 0–30 MeV analysis.

Making all these adjustments to the complete data set results in a total number of 291 data to be rejected, leaving us with our final data set of 1626 scattering observables divided over 213 groups, as presented in Table I. Of these groups 117 have an experimental normalization error and 22 groups have a floated normalization. Each group of Zürich78 cross-section data[28] contains two angle-dependent normalization data. Including the 27

P-matrix parameters and the pion-nucleon coupling constant, we are left with a total number of degrees of freedom of $N_{df} = 1576$. The parameter f^s_{med} and the boundary condition radius were fixed at $f^s_{med} = 1.6$ and $b = 1.4$ fm in our final ME fit and we do not count them as free parameters.

VI. RESULTS

Starting with the complete data set of 1917 pp scattering observables, the 27 P-matrix parameters, the pion-nucleon coupling constant f_0^2, the free parameter f_{med}, indicating the strength of the HBE potential tail outside $r = b$, were adjusted to obtain the best possible description of the data. The boundary condition radius is set at $b = 1.4$ fm. Of the data, 291 did not survive our rejection criteria, so our final data set contains 1626 scattering observables (with an additional 129 normalization data). The parameter f_{med} was found to be helpful in the singlet partial waves only and was fixed in our final ME fit to be $f^s_{med} = 1.6$.

Taking into account all free parameters, floated normalizations and other normalization errors, we are left with a total number of degrees of freedom of $N_{df} = 1576$. Our minimum χ^2 value is $\chi^2_{min} = 1760.6$ if we include the magnetic-moment interaction and $\chi^2_{min} = 1789.2$ if we do not include it, which means a five standard deviation effect. We do not find a significant difference in χ^2_{min} if we replace the momentum dependent (dipole) proton form factors by their point particle approximation, which is not surprising in view of the short-range effect of this momentum dependence. We obtain $\chi^2/N_{df} = 1.117$ for the analysis with the magnetic-moment interaction included, and $\chi^2/N_{dat} = 1.003$, where $N_{dat} = 1755$ is the number of data points (scattering observables and normalization errors). This is lower than any other phase-shift analysis.[6,7,18-20]

The $pp\pi^0$ pseudovector coupling constant is found to be

$$f_0^2 = (74.9 \pm 0.7) \times 10^{-3} \text{ or } g_0^2 = 13.55 \pm 0.13 ,$$

where

$$g_0^2 = (2M_p/m_c)^2 f_0^2 = 180.78 f_0^2 .$$

TABLE III. P-matrix parameters for the parametrized waves (see text).

	c_0	c_1	c_2	c_3	c_4	c_5	c_6
$^1S_0$	-0.853	0.185	-0.201	0.390	-0.194	0.040	-0.003
$^3P_0$	2.782	-0.322	0.103	0	0	0	0
$^3P_1$	2.738	0.783	-0.248	0.033	0	0	0
$^1D_2$	1.348	-0.363	-0.014	0	0	0	0
$P_1 \ (J=2)$	-1.123	-0.024	-0.014	0	0	0	0
$\theta \ (J=2)$	0.011	0.014	0	0	0	0	0
$P_2 \ (J=2)$	1.334	0	0	0	0	0	0
$^3F_3$	-0.825	0	0	0	0	0	0
$P_1 \ (J=4)$	-4.700	0.885	0	0	0	0	0
$\theta \ (J=4)$	0	0	0	0	0	0	0
$P_2 \ (J=4)$	0	0	0	0	0	0	0
$^1G_4$	15.097	0	0	0	0	0	0

TABLE IV. SE results at ten energy clusters. N_{obs}: number of scattering observables. N_{df}: number of degrees of freedom. The phase parameters in degrees are with respect to EM wave functions and the SE error is the square root of the diagonal elements of the full error matrix. δ^C_{C+EM} denotes the EM phase shift.

0.382 54 MeV	N_{obs}	N_{df}	χ^2_{ME}	χ^2_{SE}
	122	118	139.82	134.09
Phase	ME	SE	Error (SE)	δ^C_{C+EM}
$^1S_0$	14.6075	14.6076	0.0025	-0.0985
Δ_C	-0.0009	-0.0069	0.0025	-0.0547
1.0 MeV	N_{obs}	N_{df}	χ^2_{ME}	χ^2_{SE}
	57	55	42.30	38.08
Phase	ME	SE	Error (SE)	δ^C_{C+EM}
$^1S_0$	32.6667	32.6813	0.0094	-0.0805
Δ_C	-0.0045	-0.0096	0.0029	-0.0503
5.0 MeV	N_{obs}	N_{df}	χ^2_{ME}	χ^2_{SE}
	45	40	38.48	30.74
Phase	ME	SE	Error (SE)	δ^C_{C+EM}
$^1S_0$	54.7423	54.5464	0.0871	-0.0376
$^3P_0$	1.5793	1.6144	0.0927	-0.1248
$^3P_1$	-0.8961	-0.9072	0.0282	-0.0427
$^3P_2$	0.2129	0.2272	0.0177	-0.0153
$^1D_2$	0.0433	0.0395	0.0096	-0.0282
10.0 MeV	N_{obs}	N_{df}	χ^2_{ME}	χ^2_{SE}
	103	97	103.54	86.68
Phase	ME	SE	Error (SE)	δ^C_{C+EM}
$^1S_0$	55.1273	55.0896	0.0681	-0.0156
$^3P_0$	3.7222	3.5426	0.0729	-0.1546
$^3P_1$	-2.0442	-2.1048	0.0266	-0.0387
$^3P_2$	0.6462	0.6601	0.0172	0.0006
$^1D_2$	0.1645	0.1766	0.0108	-0.0246
25.0 MeV	N_{obs}	N_{df}	χ^2_{ME}	χ^2_{SE}
	56	49	62.72	60.35
Phase	ME	SE	Error (SE)	δ^C_{C+EM}
$^1S_0$	48.7039	48.8364	0.1332	0.0202
$^3P_0$	8.5542	8.4968	0.6057	-0.2082
$^3P_1$	-4.8891	-4.7272	0.1964	-0.0341
$^3P_2$	2.4749	2.3712	0.1425	0.0280
$^1D_2$	0.6898	0.7665	0.0922	-0.0209
ε_2	-0.8089	-0.9582	0.1303	0.0075
50.0 MeV	N_{obs}	N_{df}	χ^2_{ME}	χ^2_{SE}
	218	208	210.10	206.98
Phase	ME	SE	Error (SE)	δ^C_{C+EM}
$^1S_0$	39.1216	39.0859	0.1034	0.0563
$^3P_0$	11.4412	11.2540	0.3031	-0.2510
$^3P_1$	-8.2654	-8.2992	0.0480	-0.0289
$^3P_2$	5.8231	5.8834	0.0629	0.0566
$^1D_2$	1.6951	1.7153	0.0141	-0.0197
ε_2	-1.7088	-1.7186	0.0221	0.0102
100.0 MeV	N_{obs}	N_{df}	χ^2_{ME}	χ^2_{SE}
	155	143	171.64	151.25
Phase	ME	SE	Error (SE)	δ^C_{C+EM}
$^1S_0$	24.915	24.722	0.479	0.104
$^3P_0$	9.481	10.690	1.197	-0.276
$^3P_1$	-13.287	-13.429	0.236	-0.018
$^3P_2$	10.987	10.736	0.207	0.095
$^1D_2$	3.794	3.630	0.100	-0.021
ε_2	-2.650	-2.562	0.105	0.012

TABLE IV. (Continued).

$^3F_2$	0.817	1.083	0.111	−0.107

150.0 MeV	N_{obs}	N_{df}	χ^2_{ME}	χ^2_{SE}
	323	309	367.34	359.09
Phase	ME	SE	Error (SE)	δ^C_{C+EM}
$^1S_0$	14.167	14.306	0.374	0.137
$^3P_0$	4.720	4.966	0.275	−0.273
$^3P_1$	−17.517	−17.626	0.094	−0.007
$^3P_2$	13.990	13.943	0.069	0.122
$^1D_2$	5.687	5.691	0.073	−0.024
ε_2	−2.859	−2.854	0.045	0.013
$^3F_2$	1.200	1.010	0.089	−0.127
$^3F_3$	−2.101	−1.881	0.118	−0.021

215.0 MeV	N_{obs}	N_{df}	χ^2_{ME}	χ^2_{SE}
	197	184	266.88	253.00
Phase	ME	SE	Error (SE)	δ^C_{C+EM}
$^1S_0$	4.107	4.205	0.311	0.168
$^3P_0$	−1.903	−1.810	0.395	−0.258
$^3P_1$	−22.311	−22.152	0.204	0.005
$^3P_2$	16.023	15.846	0.120	0.145
$^1D_2$	7.607	7.766	0.115	−0.029
ε_2	−2.685	−2.550	0.085	0.012
$^3F_2$	1.466	1.183	0.168	−0.146
$^3F_3$	−2.576	−2.455	0.109	−0.022
$^3F_4$	1.926	1.859	0.102	0.066
$^1G_4$	1.050	0.986	0.048	−0.011
ε_4	−1.174	−1.162	0.058	0.007
$^3H_4$	0.354	0.292	0.069	−0.084

320.0 MeV	N_{obs}	N_{df}	χ^2_{ME}	χ^2_{SE}
	350	336	357.78	353.18
Phase	ME	SE	Error (SE)	δ^C_{C+EM}
$^1S_0$	−8.064	−8.142	0.349	0.200
$^3P_0$	−12.364	−12.495	0.468	−0.228
$^3P_1$	−29.107	−29.292	0.292	0.019
$^3P_2$	17.368	17.508	0.133	0.166
$^1D_2$	9.879	9.871	0.115	−0.035
ε_2	−2.290	−2.410	0.094	0.009
$^3F_2$	1.257	1.321	0.160	−0.168
$^3F_3$	−2.883	−2.919	0.113	−0.023
$^3F_4$	3.094	3.056	0.091	0.082
$^1G_4$	1.553	1.565	0.065	−0.012
ε_4	−1.523	−1.557	0.051	0.007
$^3H_4$	0.561	0.674	0.079	−0.100

This result is slightly higher than our previously published value of $f_0^2 = (72.5\pm0.6)\times10^{-3}$, or $g_0^2 = 13.1\pm0.1$, obtained from our preliminary earlier phase-shift analysis.[2] However, that analysis did not contain the magnetic-moment interaction. Because of its long range, the magnetic-moment interaction is likely to influence the value of f_0^2, so we have to compare the result with the result from the analysis without the magnetic-moment interaction. This analysis now yields

$$f_0^2 = (73.7\pm0.7)\times10^{-3} ,$$

or $g_0^2 = 13.33\pm0.13$, in good agreement with our preliminary analysis.[2]

The result for f_0^2 is in reasonable agreement with earlier (less accurate) determinations (see Table II), except

for the value obtained by Kroll.[133] It differs, however, by more than three standard deviations from the value for the charged coupling constant as determined from πN scattering[26]

$$f_c^2 = (78.9\pm1.0)\times10^{-3}$$

or $g_c^2 = 14.28\pm0.18$, where

$$g_c^2 = [(M_p + M_n)/m_c]^2 f_c^2 = 181.03 f_c^2 .$$

For charge independence [SU(2)-isospin symmetry] of the pion-nucleon interaction one has $f_0^2 = f_c^2$, so our determination of the $pp\pi^0$ coupling constant seems to indicate a large breaking of charge independence.

Introducing different coupling constants for the spin

triplets f_T and for the spin singlets f_S, we obtain

$$f_S^2 = (76.0 \pm 1.3) \times 10^{-3}$$

and

$$f_T^2 = (74.8 \pm 0.7) \times 10^{-3} \ ,$$

indicating the importance of the spin-triplet waves in the determination. When we next introduce different coupling constants for the ^3P waves $f(^3P)$ and all other partial waves f (rest), we find

$$f(^3P)^2 = (74.7 \pm 0.8) \times 10^{-3}$$

and

$$f(\mathrm{rest})^2 = (75.1 \pm 0.7) \times 10^{-3} \ ,$$

indicating that the ^3P waves are not especially important in the determination of the coupling constant. It is therefore not possible for us to pinpoint some special type of observables as being responsible for the low value of f_0^2. It rather appears that the data as a whole require a low pion-nucleon coupling constant.

The multienergy results for each group of data is given in Table I. There we give the χ^2-values, the predicted

normalization with which the experimental data should be multiplied before comparing them with the theoretical values, which data were rejected, and why they were rejected.

The phase parameters were parametrized with 27 P-matrix parameters. For the P-matrix parametrization we used an energy-dependent potential, independent of r for $r < b$ [Eqs. (8) and (11)]. We allow for up to seven parameters in each partial wave (i.e., up to sixth order in k^2), which was found to be enough (only the $^1S_0$ required all seven parameters). The resulting coefficients as obtained in our final ME fit are presented in Table III. The coefficients c_n have dimension [fm^{2n}] and are related to the coefficients of Eq. (9) according to $a_n = c_n/b^2$, i.e., the corresponding energy-dependent potential in MeV is obtained by multiplying with $1/M_p b^2 = 21.173$ MeV. The ME phase parameters were used in the computer code SAID (Ref. 123) to provide an objective criterion for the quality of our results. For 1083 data in the energy range 3–325 MeV this results in $\chi^2 = 1092.2$ or $\chi^2/N_{\mathrm{dat}} = 1.01$, in excellent agreement with the result of our own phase-shift analysis of $\chi^2/N_{\mathrm{dat}} = 1.02$ in the same energy range.

Single-energy phase-shift analyses were performed by fitting a constant to the P-matrix parametrization (which
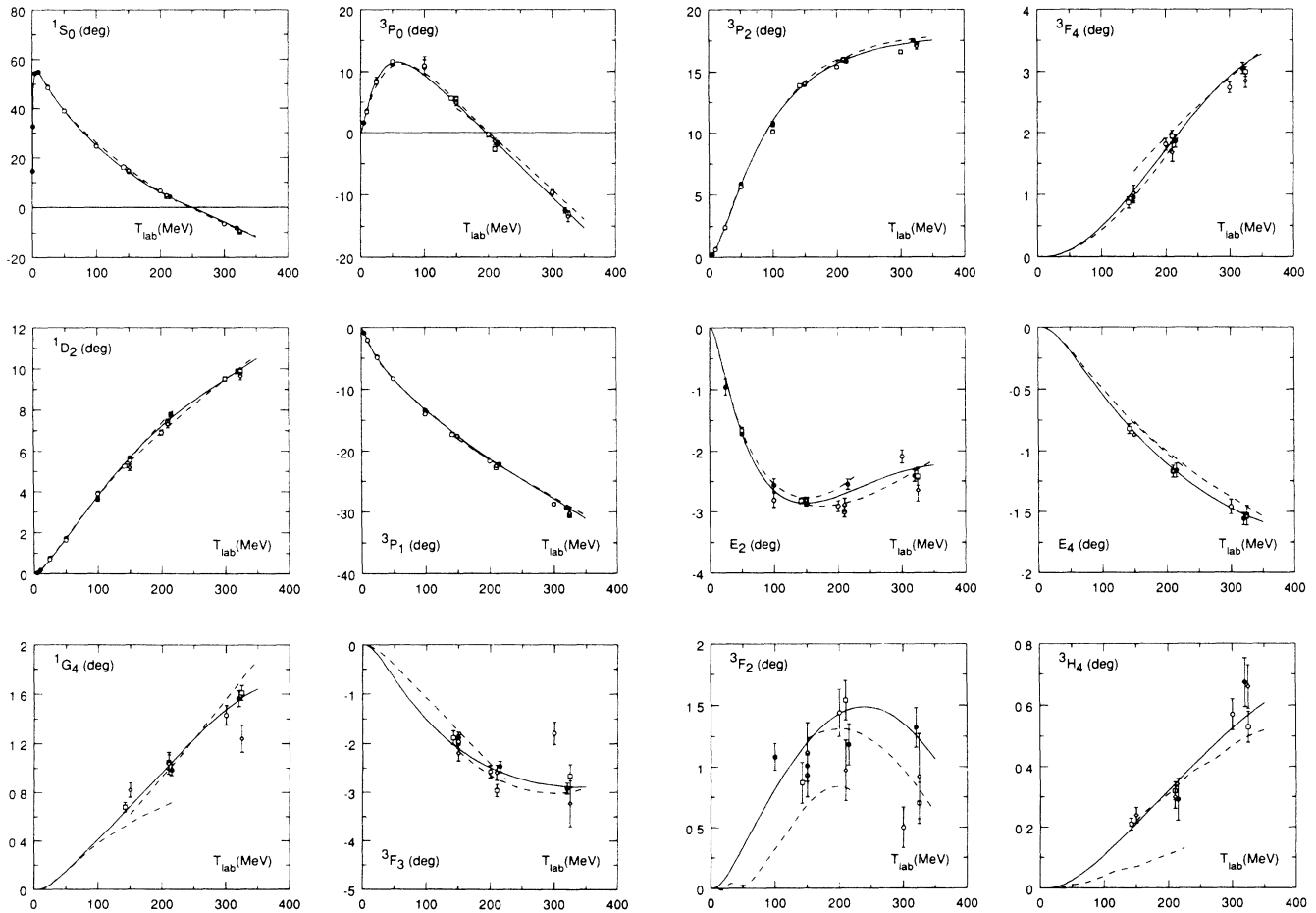

FIG. 1. Phase shifts in degrees vs T_{lab} in MeV. Errors are shown only if they are large enough to be plotted. Solid line: multienergy analysis; dashed line: Bystricky *et al.* (Ref. 6). ●: single-energy analysis; ○: Arndt *et al.* (Ref. 7); □: Dubois *et al.* (Ref. 18); ◇: Bugg *et al.* (Ref. 19).

was now held fixed at the ME result in order to insure the proper local energy behavior) for all phase parameters that were to be determined. The SE analyses were performed at ten different energies from 0.382 54 (the interference minimum) to 320 MeV. The data were divided into ten groups and clustered around the appropriate energies. The results are presented in Table IV, where we give the ME χ^2, the ME phase parameters, the SE χ^2, and the SE phase parameters with their errors. The errors are the square roots of the diagonal elements of the inverse of one half times the second derivative matrix of χ^2 with respect to the parameters (the error matrix). Actually, all phase parameters within a SE analysis are correlated with each other, so instead of the error as presented in Table IV, one should use the complete error matrix whenever one wants to determine quantities derived from a combination of phase parameters. Since these error matrices become larger with the number of searched phase parameters (12×12 matrices for the SE analyses at 215 and 320 MeV) we do not reproduce them here because of lack of space. They are available upon request. The agreement between the ME and SE phase parameters is good, which validates our procedure of using the energy slopes from the ME analysis when doing the single-energy analysis.

The phase parameters are phase shifts and mixing parameters with respect to electromagnetic (EM) wave functions (δ^{C+EM}_{C+EM+N} in the notation of Ref. 1). They can be converted to phase shifts with respect to Coulomb functions by subtracting the EM phase shifts δ^{C}_{C+EM}, which contain the contributions of the relativistic Coulomb interaction, the magnetic-moment interaction with dipole form factors, and the vacuum polarization. Since the magnetic-moment interaction contains a tensor part [see Eq. (13)] one should use the S matrix whenever one wants to convert the triplet coupled phase parameters with respect to EM wave functions to phase parameters with respect to Coulomb functions, i.e.,

$$S^{C}_{C+EM+N} = (S^{C}_{C+EM})^{1/2} S^{C+EM}_{C+EM+N} (S^{C}_{C+EM})^{1/2} .$$

Doing this results in the corrections δ^{C}_{C+EM} for each phase parameter separately as given in Table IV. The phase parameters can then be compared with the results of our 0–30 MeV analysis.[1] The differences remain well within one standard deviation for most phase parameters.

Table IV furthermore contains the number of scattering observables and the number of degrees of freedom for each SE analysis.

The ME phase parameters are shown in Fig. 1 together with the results of the phase-shift analyses of Arndt, Hyslop, and Roper,[7] Bystricky, Lechanoine-Leluc, and Lehar,[6] Dubois et al.,[18] and Bugg et al.[19] All phase parameters can be determined rather accurately and compare favorably with the other phase-shift analyses. However, we think that our phase parameters are more in accordance with the data because of our considerably lower value of χ^2/N_{df} as compared to, e.g., Arndt[7] ($\chi^2/N_{df} = 1.3$). Furthermore, the bulk of new data of Onel et al.[103] at 241, 314, and 341 MeV, which have not been used in previous phase-shift analyses, provide important constraints on the phase parameters at higher en-
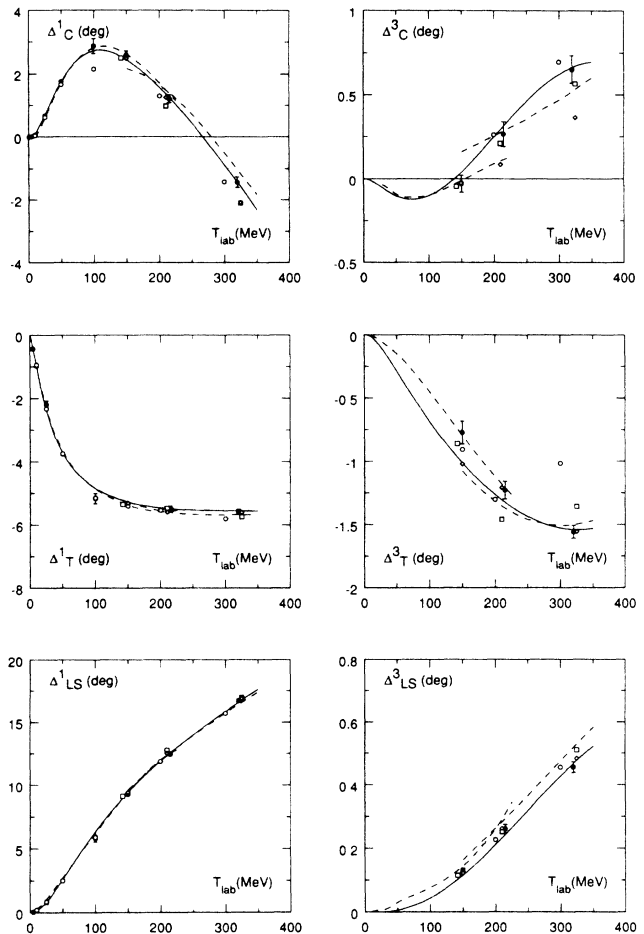

FIG. 2. Phase-shift combinations of ^3P and ^3F waves in degrees vs T_{lab} in MeV. Errors are shown for our SE results (bullets) only. Curves and symbols have the same meaning as in Fig. 1.

ergies. Especially the ^3F phase shifts above 200 MeV, that can now be determined more accurately than in previous analyses. The differences with, e.g., Arndt are most strikingly seen in the $^3F_2$ and $^3F_3$ phase shifts at 300 MeV.

The central, tensor, and spin-orbit combinations of the P and F waves are shown in Fig. 2. The SE results are given with their error bars, whereas the other analyses do not publish error bars for their combined phase parameters. The spin-orbit combinations of both P and F waves are determined very accurately.

VII. SUMMARY

Summarizing, we have performed a phase-shift analysis of all pp scattering data below $T_{lab} = 350$ MeV, published in a regular physics journal as of 1955. The total data set contains 1917 scattering data of which 291 do not survive our rejection criteria. The final data set contains 1626 scattering observables and 129 normalization data. With 27 P-matrix parameters and the $pp\pi^0$ coupling constant we arrive at $\chi^2/N_{df} = 1.117$, which is lower than any oth-

er phase-shift analysis.

Our method for analyzing the data allows us to determine the $pp\pi^0$ coupling constant at the pion pole and we find $f_0^2 = (74.9 \pm 0.7) \times 10^{-3}$. This result is significantly different from the charged pion-nucleon coupling constant $f_c^2 = (78.9 \pm 1.0) \times 10^{-3}$, indicating a large breaking of charge independence in the nucleon-nucleon interaction. More conclusive evidence for such a large breaking would be obtained if both neutral and charged coupling constants could be determined in a combined pp and np phase-shift analysis of all NN scattering data below $T_{lab} = 350$ MeV. This is under investigation.

The present results will serve as a basis for our future NN phase-shift analyses. Some of the results of our np phase-shift analysis below $T_{lab} = 30$ MeV have already been published,[136,137] and the 0–350 MeV np analysis is in progress. The next step will be to extend our analyses to energies above the threshold by including inelasticities.

*Electronic mail: U634999 at HNYKUN11.BITNET.

[1] J. R. Bergervoet, P. C. van Campen, W. A. van der Sanden, and J. J. de Swart, Phys. Rev. C 38, 15 (1988).

[2] J. R. Bergervoet, P. C. van Campen, T. A. Rijken, and J. J. de Swart, Phys. Rev. Lett. 59, 2255 (1987).

[3] J. R. Bergervoet, P. C. van Campen, T. A. Rijken, and J. J. de Swart, Phys. Rev. C 38, 770 (1988).

[4] G. J. M. Austen and J. J. de Swart, Phys. Rev. Lett. 50, 2039 (1983).

[5] L. Durand III, Phys. Rev. 108, 1597 (1957).

[6] J. Bystricky, C. Lechanoine-Leluc, and F. Lehar, J. Phys. (Paris) 48, 199 (1987).

[7] R. A. Arndt, J. S. Hyslop III, and L. D. Roper, Phys. Rev. D 35, 128 (1987).

[8] M. M. Nagels, T. A. Rijken, and J. J. de Swart, Phys. Rev. D 17, 768 (1978).

[9] R. L. Jaffe and F. E. Low, Phys. Rev. D 19, 2105 (1979).

[10] M. Lacombe, B. Loiseau, J. M. Richard, R. Vinh Mau, J. Côté, P. Pirès, and R. de Tourreil, Phys. Rev. C 21, 861 (1980).

[11] M. H. Partovi and E. L. Lomon, Phys. Rev. D 2, 1999 (1970); K. Erkelenz, Phys. Rep. 13C, 191 (1974); J. J. de Swart and M. M. Nagels, Fortschr. Phys. 26, 215 (1978).

[12] A. A. Logunov and A. N. Tavkhelidze, Nuovo Cimento 29, 380 (1963); R. Blankenbecler and R. Sugar, Phys. Rev. 142, 1051 (1966); V. G. Kadyshevsky, Nucl. Phys. B6, 125 (1968); Nuovo Cimento 55, 275 (1968).

[13] H. P. Stapp, T. J. Ypsilantis, and N. Metropolis, Phys. Rev. 105, 302 (1957).

[14] R. E. Cutkosky and B. B. Deo, Phys. Rev. 174, 1859 (1968).

[15] S. Ciulli, Nuovo Cimento A 61, 787 (1969); 62, 301 (1969).

[16] M. H. MacGregor, M. J. Moravcsik, and H. P. Stapp, Annu. Rev. Nucl. Sci. 10, 291 (1960).

[17] N. Hoshizaki, Prog. Theor. Phys. Suppl. 42, 107 (1968).

[18] R. Dubois, D. Axen, R. Keeler, M. Comyn, G. A. Ludgate, J. R. Richardson, N. M. Stewart, A. S. Clough, D. V. Bugg, and J. A. Edgington, Nucl. Phys. A377, 554 (1982).

[19] D. V. Bugg, J. A. Edgington, C. Amsler, R. C. Brown, C. J. Oram, K. Shakarchi, N. M. Stewart, G. A. Ludgate, A. S. Clough, D. Axen, S. Jaccard, and J. Vávra, J. Phys. G 4, 1025 (1978).

[20] R. A. Arndt, L. D. Roper, R. A. Bryan, R. B. Clark, B. J. VerWest, and P. Signell, Phys. Rev. D 28, 97 (1983).

[21] J. J. de Swart, W. A. van der Sanden, and W. Derks, Nucl. Phys. A416, 299c (1984).

[22] V. G. J. Stoks and J. J. de Swart (unpublished).

[23] G. Breit, Phys. Rev. 99, 1581 (1955).

[24] R. Hofstadter, F. Bumiller, and M. R. Yearian, Rev. Mod.

Phys. 30, 482 (1958).

[25] L. D. Knutson and D. Chiang, Phys. Rev. C 18, 1958 (1978).

[26] O. Dumbrajs, R. Koch, H. Pilkuhn, G. C. Oades, H. Behrens, J. J. de Swart, and P. Kroll, Nucl. Phys. B216, 277 (1983).

[27] J. E. Brolley, Jr., J. D. Seagrave, and J. G. Beery, Phys. Rev. 135, B1119 (1964); M. L. Gursky and L. Heller, *ibid.* 136, B1693 (1964).

[28] Ch. Thomann, J. E. Benn, and S. Münch, Nucl. Phys. A303, 457 (1978).

[29] H. Wassmer and H. Mühry, Helv. Phys. Acta 46, 626 (1973).

[30] J. Birchall, E. Baumgartner, H. M. Friess, H. Mühry, F. Rösel, and D. Trautmann, Helv. Phys. Acta 50, 509 (1977).

[31] D. J. Knecht, P. F. Dahl, and S. Messelt, Phys. Rev. 148, 1031 (1966).

[32] K. Imai, K. Nisimura, N. Tamura, and H. Sato, Nucl. Phys. A246, 76 (1975).

[33] M. D. Barker, P. C. Colby, W. Haeberli, and P. Signell, Phys. Rev. Lett. 48, 918 (1982); 49, 1056E (1982).

[34] R. J. Slobodrian, H. E. Conzett, E. Shield, and W. F. Tivol, Phys. Rev. 174, 1122 (1968).

[35] G. Bittner and W. Kretschmer, Phys. Rev. Lett. 43, 330 (1979).

[36] H. Obermeyer, H. Kuiper, B. Seidler, and K. Frank, Nucl. Phys. A344, 75 (1980).

[37] R. J. Slobodrian, J. S. C. McKee, H. Bichsel, and W. F. Tivol, Phys. Rev. Lett. 19, 704 (1967).

[38] L. H. Johnston and D. E. Young, Phys. Rev. 116, 989 (1959).

[39] N. Jarmie, R. E. Brown, R. L. Hutson, and J. L. Detch, Jr., Phys. Rev. Lett. 24, 240 (1970); N. Jarmie, J. H. Jett, J. L. Detch, Jr., and R. L. Hutson, *ibid.* 25, 34 (1970).

[40] J. D. Hutton, W. Haeberli, L. D. Knutson, and P. Signell, Phys. Rev. Lett. 35, 429 (1975).

[41] P. Catillon, M. Chapellier, and D. Garreta, Nucl. Phys. B2, 93 (1967).

[42] S. Kikuchi, J. Sanada, S. Suwa, I. Hayashi, K. Nisimura, and K. Fukunaga, J. Phys. Soc. Jpn. 15, 9 (1960).

[43] W. A. Blanpied, Phys. Rev. 116, 738 (1959).

[44] K. W. Brockman, Jr., Phys. Rev. 110, 163 (1958).

[45] N. Jarmie and J. H. Jett, Phys. Rev. C 13, 2554 (1976).

[46] J. W. Burkig, J. R. Richardson, and G. E. Schrank, Phys. Rev. 113, 290 (1959).

[47] H. N. Royden and B. T. Wright, Phys. Rev. 113, 294 (1959).

[48] A. Abragam, M. Borghini, P. Catillon, J. Coustham, P. Roubeau, and J. Thirion, Phys. Lett. 2, 310 (1962).

[49] P. Catillon, J. Sura, and A. Tarrats, Phys. Rev. Lett. 20, 602 (1968).

[50] C. J. Batty, G. H. Stafford, and R. S. Gilmore, Nucl. Phys. 51, 225 (1964).

[51]T. H. Jeong, L. H. Johnston, D. E. Young, and C. N. Waddell, Phys. Rev. 118, 1080 (1960).

[52]N. Jarmie, J. E. Brolley, H. Kruse, H. C. Bryant, and R. Smythe, Phys. Rev. 155, 1438 (1967).

[53]P. Christmas and A. E. Taylor, Nucl. Phys. 41, 388 (1963).

[54]A. Ashmore, B. W. Davies, M. Devine, S. J. Hoey, J. Litt, M. E. Shepherd, R. C. Hanna, and L. P. Robertson, Nucl. Phys. 73, 256 (1965).

[55]L. H. Johnston and Y. S. Tsai, Phys. Rev. 115, 1293 (1959).

[56]C. J. Batty, R. S. Gilmore, and G. H. Stafford, Nucl. Phys. 45, 481 (1963).

[57]D. Garreta, K. Nisimura, and M. Fruneau, Phys. Lett. 31B, 363 (1970).

[58]L. H. Johnston and D. A. Swenson, Phys. Rev. 111, 212 (1958).

[59]U. E. Kruse, J. M. Teem, and N. F. Ramsey, Phys. Rev. 101, 1079 (1956).

[60]J. N. Palmieri, A. M. Cormack, N. F. Ramsey, and R. Wilson, Ann. Phys. (NY) 5, 299 (1958).

[61]D. Garreta and M. Fruneau, Nucl. Phys. A170, 492 (1971).

[62]K. Nisimura, T. Hasegawa, T. Saito, E. Takasaki, N. Horikawa, T. Nakanishi, M. Saito, S. Sugimoto, T. Yamaki, and H. Ueno, Phys. Lett. 30B, 612 (1969).

[63]A. Ashmore, M. Devine, B. Hird, J. Litt, W. H. Range, M. E. Shepherd, and R. L. Clarke, Nucl. Phys. 65, 305 (1965).

[64]C. J. Batty, T. C. Griffith, D. C. Imrie, G. J. Lush, and L. A. Robbins, Nucl. Phys. A98, 489 (1967).

[65]T. C. Griffith, D. C. Imrie, G. J. Lush, and A. J. Metheringham, Phys. Rev. Lett. 10, 444 (1963).

[66]A. Berdoz, F. Foroughi, and C. Nussbaum, J. Phys. G 12, L133 (1986).

[67]K. Nisimura, J. Sanada, P. Catillon, K. Fukunaga, T. Hasegawa, H. Hasai, N. Ryu, D. C. Worth, and H. Imada, Prog. Theor. Phys. 30, 719 (1963).

[68]J. Sanada, K. Kuriyama, Y. Takeuchi, Y. Nojiri, N. Ryu, H. Hasai, M. Ikeda, S. Kobayashi, K. Nagamine, D. C. Worth, and T. Yamaya, Nucl. Phys. B4, 379 (1968).

[69]N. Tamura, K. Imai, K. Nisimura, K. Egawa, K. Hatanaka, H. Shimizu, T. Saito, H. Sato, Y. Wakuta, H. Hasuyama, Y. Mori, and H. Yamamoto, J. Phys. Soc. Jpn. 44, S289 (1978).

[70]D. E. Young and L. H. Johnston, Phys. Rev. 119, 313 (1960).

[71]O. N. Jarvis, T. W. P. Brogden, B. Rose, J. P. Scanlon, J. Orchard-Webb, and M. R. Wigan, Nucl. Phys. A108, 63 (1968).

[72]M. R. Wigan, R. A. Bell, P. J. Martin, O. N. Jarvis, and J. P. Scanlon, Nucl. Phys. A114, 377 (1968).

[73]A. E. Taylor, E. Wood, and L. Bird, Nucl. Phys. 16, 320 (1960).

[74]E. H. Thorndike and T. R. Ophel, Phys. Rev. 119, 362 (1960).

[75]O. N. Jarvis, B. Rose, G. F. Cox, and G. H. Eaton, Nucl. Phys. 61, 194 (1965).

[76]E. Baskir, E. M. Hafner, A. Roberts, and J. H. Tinlot, Phys. Rev. 106, 564 (1957).

[77]S. Hee and R. Wilson, Phys. Rev. 132, 2236 (1963).

[78]C. Caverzasio, A. Michalowicz, K. Kuroda, M. Poulet, and N. Poutcherov, J. Phys. Radium 24, 1048 (1963).

[79]S. Hee and E. H. Thorndike, Phys. Rev. 132, 744 (1963).

[80]O. N. Jarvis, B. Rose, G. H. Eaton, and C. P. van Zyl, Nucl. Phys. 50, 529 (1964).

[81]E. H. Thorndike, J. Lefrançois, and R. Wilson, Phys. Rev. 120, 1819 (1960).

[82]G. F. Cox, G. H. Eaton, C. P. van Zyl, O. N. Jarvis, and B. Rose, Nucl. Phys. B4, 353 (1967).

[83]L. Bird, D. N. Edwards, B. Rose, A. E. Taylor, and E. Wood, Nucl. Phys. 42, 280 (1963).

[84]C. F. Hwang, T. R. Ophel, E. H. Thorndike, and R. Wilson, Phys. Rev. 119, 352 (1960).

[85]L. Bird, P. Christmas, A. E. Taylor, and E. Wood, Nucl. Phys. 27, 586 (1961).

[86]O. N. Jarvis, B. Rose, J. P. Scanlon, and E. Wood, Nucl. Phys. 42, 294 (1963).

[87]O. N. Jarvis, C. Whitehead, and M. Shah, Phys. Lett. 36B, 409 (1971).

[88]J. M. Cassels, Proc. Phys. Soc. London, Sect. A 69, 495 (1956).

[89]A. Michalowicz, Rev. Mod. Phys. 39, 523 (1967).

[90]O. Chamberlain and J. D. Garrison, Phys. Rev. 103, 1860 (1956).

[91]D. Fischer and J. Baldwin, Phys. Rev. 100, 1445 (1955).

[92]P. Hillman, A. Johansson, and G. Tibell, Phys. Rev. 110, 1218 (1958).

[93]B. A. Ryan, A. Kanofsky, T. J. Devlin, R. E. Mischke, and P. F. Shepard, Phys. Rev. D 3, 1 (1971).

[94]L. G. Greeniaus, D. A. Hutcheon, C. A. Miller, G. A. Moss, G. Roy, R. Dubois, C. Amsler, B. K. S. Koene, and B. T. Murdoch, Nucl. Phys. A322, 308 (1979).

[95]D. Axen, L. Felawka, S. Jaccard, J. Vávra, G. A. Ludgate, N. M. Stewart, C. Amsler, R. C. Brown, D. V. Bugg, J. A. Edgington, C. J. Oram, K. Shakarchi, and A. S. Clough, Lett. Nuovo Cimento 20, 151 (1977).

[96]E. H. Thorndike, Rev. Mod. Phys. 39, 513 (1967).

[97]A. Abashian and E. M. Hafner, Phys. Rev. Lett. 1, 255 (1958).

[98]J. H. Tinlot and R. E. Warner, Phys. Rev. 124, 890 (1961).

[99]J. F. Marshall, C. N. Brown, and F. Lobkowicz, Phys. Rev. 150, 1119 (1966).

[100]K. Gotow, F. Lobkowicz, and E. Heer, Phys. Rev. 127, 2206 (1962).

[101]A. C. England, W. A. Gibson, K. Gotow, E. Heer, and J. Tinlot, Phys. Rev. 124, 561 (1961).

[102]K. Gotow and F. Lobkowicz, Phys. Rev. 136, B1345 (1964).

[103]Y. Onel, R. Hausammann, E. Heer, R. Hess, C. Lechanoine-Leluc, W. R. Leo, D. Rapin, S. Jaccard, and S. Mango, Phys. Rev. D 40, 35 (1989).

[104]C. Amsler, D. Axen, J. Beveridge, D. V. Bugg, A. S. Clough, R. Dubois, J. A. Edgington, D. Gibson, R. Keeler, G. A. Ludgate, C. J. Oram, J. R. Richardson, L. P. Robertson, and N. M. Stewart, J. Phys. G 4, 1047 (1978).

[105]O. Chamberlain, E. Segrè, R. D. Tripp, C. Wiegand, and T. Ypsilantis, Phys. Rev. 105, 288 (1957).

[106]D. Aebischer, B. Favier, L. G. Greeniaus, R. Hess, A. Junod, C. Lechanoine, J. C. Niklès, D. Rapin, C. Richard-Serre, and D. W. Werren, Phys. Rev. D 13, 2478 (1976).

[107]D. Ottewell, P. Walden, E. G. Auld, G. Giles, G. Jones, G. J. Lolos, B. J. McParland, W. Ziegler, and W. Falk, Nucl. Phys. A412, 189 (1984).

[108]I. P. Auer, W. R. Ditzler, D. Hill, K. Imai, H. Spinka, R. Stanek, K. Toshioka, D. Underwood, R. Wagner, A. Yokosawa, E. W. Hoffman, J. J. Jarmer, G. R. Burleson, W. B. Cottingame, S. J. Greene, and S. Stuart, Phys. Rev. D 29, 2435 (1984).

[109]A. Beretvas, Phys. Rev. 171, 1392 (1968).

[110]D. Cheng, B. Macdonald, J. A. Helland, and P. M. Ogden, Phys. Rev. 163, 1470 (1967).

[111]D. Besset, Q. H. Do, B. Favier, L. G. Greeniaus, R. Hess, C. Lechanoine, D. Rapin, D. W. Werren, and Ch. Weddigen, Phys. Rev. D 21, 580 (1980).

[112]I. M. Vasilevskii, V. V. Vishnyakov, E. Iliesku, and A. A. Tyapkin, Zh. Eksp. Teor. Fiz. 45, 474 (1963) [Sov. Phys.—JETP 18, 327 (1964)].

[113]Yu. M. Kazarinov, F. Lehar, G. Peter, A. F. Pisarev, and K. M. Vahlbruch, Zh. Eksp. Teor. Fiz. **47**, 848 (1964) [Sov. Phys.—JETP **20**, 565 (1965)].

[114]J. E. Simmons, Phys. Rev. **104**, 416 (1956).

[115]M. W. McNaughton and E. P. Chamberlin, Phys. Rev. C **24**, 1778 (1981).

[116]J. V. Allaby, A. Ashmore, A. N. Diddens, J. Eades, G. B. Huxtable, and K. Skarsvåg, Proc. Phys. Soc. London **77**, 234 (1961).

[117]F. Shimizu, H. Koiso, Y. Kubota, F. Sai, S. Sakamoto, and S. S. Yamamoto, Nucl. Phys. **A389**, 445 (1982).

[118]F. Betz, J. Arens, O. Chamberlain, H. Dost, P. Grannis, M. Hansroul, L. Holloway, C. Schultz, and G. Shapiro, Phys. Rev. **148**, 1289 (1966).

[119]K. Abe, B. A. Barnett, J. H. Goldman, A. T. Laasanen, P. H. Steinberg, G. J. Marmer, D. R. Moffett, and E. F. Parker, Phys. Rev. D **12**, 1 (1975).

[120]M. G. Albrow, S. Andersson/Almehed, B. Bošnjaković, C. Daum, F. C. Erné, J. P. Lagnaux, J. C. Sens, and F. Udo, Nucl. Phys. **B23**, 445 (1970).

[121]J. Bystricky and F. Lehar, *Nucleon-Nucleon Scattering Data,* Vol. 11-1 of *Physics Data,* edited by H. Behrens and G. Ebel (Fachinformationszentrum, Karlsruhe, Federal Republic of Germany, 1978).

[122]J. Bystricky and F. Lehar, *Nucleon-Nucleon Scattering Data,* Vol. 11-3 of *Physics Data,* edited by H. Behrens and G. Ebel (Fachinformationszentrum, Karlsruhe, Federal Republic of Germany, 1981).

[123]Scattering Analysis Interactive Dial-up (SAID), Virginia Polytechnic Institute, Blacksburg, Virginia (R. A. Arndt, private communication).

[124]M. S. Sher, P. Signell, and L. Heller, Ann. Phys. (NY) **58**, 1 (1970).

[125]W. A. van der Sanden, A. H. Emmen, and J. J. de Swart, Institution Report No. THEF-NYM-83.11, Nijmegen, 1983 (unpublished).

[126]O. N. Jarvis and B. Rose, Phys. Lett. **15**, 271 (1965).

[127]J. Bystricky, F. Lehar, and P. Winternitz, J. Phys. (Paris) **39**, 1 (1978).

[128]M. H. MacGregor, R. A. Arndt, and R. M. Wright, Phys. Rev. **169**, 1128 (1968).

[129]M. H. MacGregor, R. A. Arndt, and R. M. Wright, Phys. Rev. **182**, 1714 (1969).

[130]R. A. Arndt, R. H. Hackman, and L. D. Roper, Phys. Rev. C **9**, 555 (1974).

[131]R. A. Arndt, R. H. Hackman, and L. D. Roper, Phys. Rev. C **15**, 1002 (1977).

[132]J. L. Yntema and M. G. White, Phys. Rev. **95**, 1226 (1954).

[133]P. Kroll, *Phenomenological Analysis of Nucleon-Nucleon Scattering,* Vol. 22-1 of *Physics Data,* edited by H. Behrens and G. Ebel (Fachinformationszentrum, Karlsruhe, Federal Republic of Germany, 1981).

[134]D. V. Bugg, Nucl. Phys. **B5**, 29 (1968).

[135]G. Breit, M. Tischler, S. Mukherjee, and J. Lucas, Proc. Nat. Acad. Sci. USA **68**, 897 (1971).

[136]V. G. J. Stoks, P. C. van Campen, W. Spit, and J. J. de Swart, Phys. Rev. Lett. **60**, 1932 (1988).

[137]V. G. J. Stoks, P. C. van Campen, T. A. Rijken, and J. J. de Swart, Phys. Rev. Lett. **61**, 1702 (1988).